Search for long-term radiation trends in the environs of Swiss nuclear power plants

B. Bucher[1], L. Rybach[2], G. Schwarz[1]

1) Swiss Federal Nuclear Safety Inspectorate, CH-5232 Villigen-HSK, Switzerland
2) Institute of Geophysics ETH Zurich, Schafmattstr. 30, CH-8093 Zurich, Switzerland

Abstract

Annually since 1989, biannually since 1994 the sites of the Swiss nuclear facilities are surveyed flying the same survey lines by airborne gamma ray spectrometry. The equipment and the data processing software used for those surveys was built and developed at the Institute of Geophysics, ETH Zurich. For mapping the ground radiation around the nuclear facilities a pixel representation and a modified Spectrum Dose Index (SDI) method is used. In the search for long-term trends the local dose-rates are calculated first and in turn the net dose rates. So far no change in the radiation levels was detected over the last 13 years outside of the fenced sites of the nuclear facilities and, especially, no artificial radioactivity was present that could not be explained by nuclear weapon tests or by the Chernobyl event.

Keywords: airborne gamma spectrometry, ground radiation, nuclear power plants, local dose rate

1. Introduction

There are five nuclear power plants at four sites in Switzerland (Beznau I+II, KKB, PWR; Mühleberg, KKM, BWR; Gösgen, KKG, PWR; Leibstadt, KKL, BWR, see Table 1) with a total generating capacity of 3.22 GWe (production in 2006: 26.2 TWh), supplying 40 % of Swiss electricity production. The Paul Scherrer Institute in Würenlingen, a renowned research facility (PSI), belongs also to the Swiss nuclear installations. Geographically the nuclear facilities are all located in the northern Alpine foreland (see Fig. 1); maps of the environs are displayed in Figures 9-11.

Table 1: The Swiss nuclear power plants.

Plant	Symbol	Type	MWe	Cooling	Since
Beznau	KKB I	PWR	365	River	1969
	KKB II	PWR	365	River	1971
Muehleberg	KKM	BWR	355	River	1972
Goesgen	KKG	PWR	970	Cooling tower	1979
Leibstadt	KKL	BWR	1165	Cooling tower	1984

The Zwischenlager Würenlingen AG (ZWILAG, interim storage facility for all categories of nuclear waste and spent fuel assemblies, in operation since 2001) is a further nuclear installation, subject to egular surveys.

The environs of the nuclear facilities are constantly monitored by local networks of ground radiation detectors and of thermoluminescence dose detectors, operated by the Swiss Federal Nuclear Safety Inspectorate (HSK).

As an additional measure, the ground radiation in the surrounding regions (approx. 50 km^2) of the nuclear power plants and of the PSI was surveyed annually since 1989 for the HSK by airborne gamma ray spectrometry (Schwarz and Rybach 1993; Rybach et al. 2000, 2001). In 1992 the measurement system has been upgraded (e.g. positioning by GPS; equipment details see below). Since 1994, the surveys are carried out with biannual frequency, within the framework of Swiss National Emergency Operation Center (NAZ) exercises. The objectives are, besides detecting of eventual releases, the establishment of baseline information (undisturbed background for reference in case of accidents), the monitoring of dose-rate distribution, and the determination of the variation width of natural radiation. The results are summarized in annual reports to the HSK and NAZ (Schwarz et al. 1989-1997, Bucher et al. 1998-2006). These reports (reports "UARM") also include descriptions of methodological developments; they can be found and downloaded from http://www.far.hsk.ch/.

Now, after more than 10 years of surveying with the new equipment, it can be investigated, whether there are some changes in the radiation levels over the time period of measurements. The measured ground radiation is expressed by dose rate ($nSvh^{-1}$), calculated by the modified Spectral Dose Index (SDI) method; details see below.

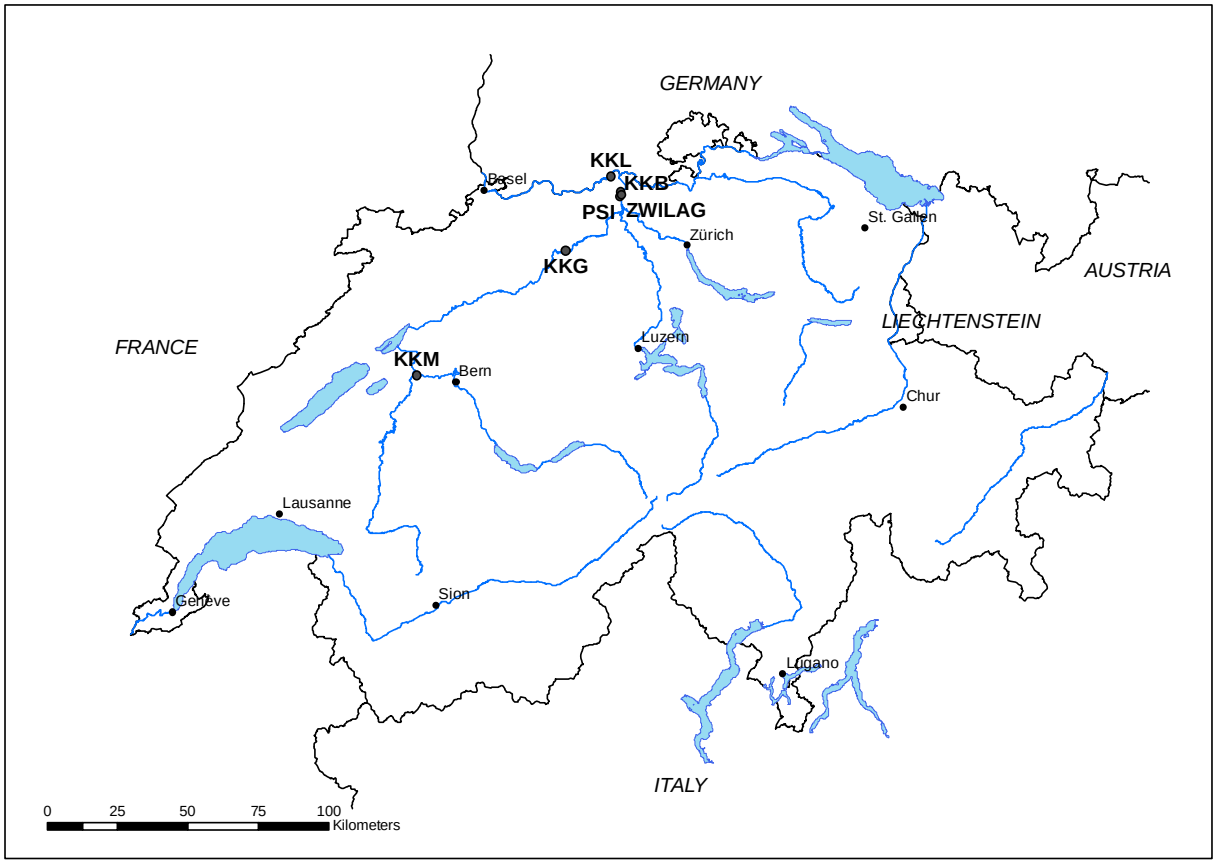

Figure 1: The locations of the Swiss nuclear facilities.

2. Equipment and calibration

The equipment used for the surveys was assembled in 1993-94 from commercial components at ETH Zurich, consisting of a 16.7 litre NaI detector, 256 channel energy stabilized

spectrometer (EXPLORANIUM 820), PC-based control with recording on memory cards (32 MBytes), and GPS navigation. Detection limit for point sources is between 0.4 and 1.9 GBq, depending on radionuclide (emitted gamma energy), vegetation cover, background and topography. The detection limit for a surface contamination by ^{137}Cs is around 0.5 to 1 kBq/m^2 depending on vegetation cover, background and topography. The detector is mounted below the helicopter and the 19“ rack with the components is mounted behind the front seat (installation time < 1 hr).

Since no concrete pads are available in or near Switzerland, calibration was done by point sources (scattering effects in ground and air considered), and at places with known ground activity. Ascending flights above large lakes and above point and volume sources yielded coefficients for data reduction (for details see Schwarz 1991 and Schwarz et al. 1997). Close agreement of ground and airborne results points towards reliable calibration (see Bucher et al. 2000).

3. Flight parameters

To have uniform coverage of the surveyed sites, the flights are carried out in a regular grid (250 m spacing between flight lines, occasional crossing lines, flight height 90 m above ground). Measurements are taken every second which corresponds to a distance of 25 m between measurements at a flight speed of 90 km/h. Super Puma helicopters of the Swiss Army are used for the flights. To make the repeated surveys comparable the same line pattern is flown each time.

Fig. 2 shows the flight lines of the 2006 survey at the KKB/KKL/PSI/ZWILAG sites.

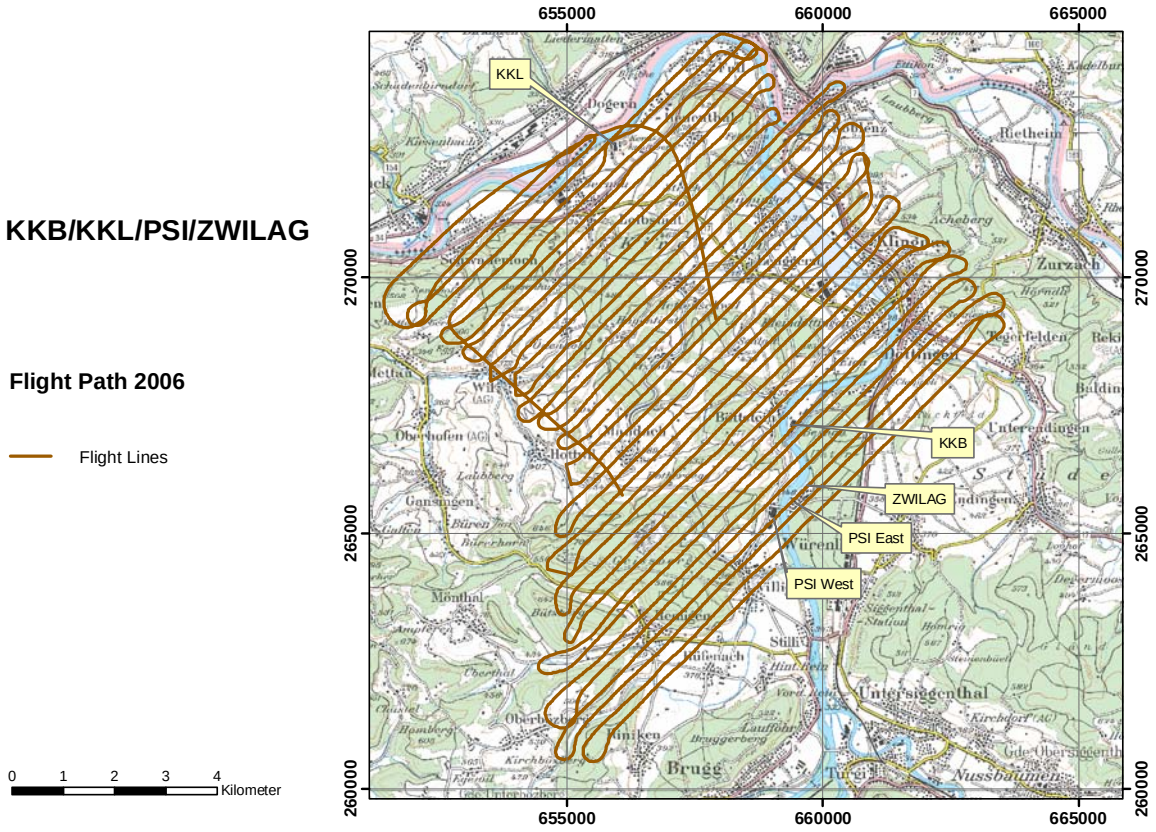

Figure 2: The flight lines of the 2006 survey at the KKB/KKL/PSI/ZWILAG sites. Swiss coordinates (km). Digital maps PK100©2003 swisstopo (DV 316.2)

4. Data processing and mapping

Data processing first performs quality control of raw data, and then in turn a series of reductions: background removal, spectral stripping, altitude/topographic correction (Schwarz et al., 1992), conversion to ground isotope concentrations, artificial radioactivity indicators, SDI-dose rate ($nSvh^{-1}$, see below), and ground dose rates. The complete processing software including modules for corrections and map output has been implemented on a laptop computer (Bucher 2001). Complete processing can thus be performed online during flights (Bucher et al. 2005). GPS positioning yields the Swiss coordinates within ± 10 m.

To keep filtering (especially when searching for weak artificial sources), to account for the relatively large measurement errors in AGS and rapidly changing radiation field intensities, the averaging pixel method is used for data representation/colour mapping (pixel size 125 x 125 m, comprises the average of five measurements; recursive nearest neighbour average interpolation). Original values are not changed by this procedure. A variety of maps can be produced: total counts, spectral windows (e.g. ^{60}Co, ^{137}Cs, ^{214}Bi for the ^{238}U series....). Three dimensional representations and ternary maps can also be produced (Schwarz and Rybach 1993, Schwarz et al. 1995).

5. Ground radiation mapping with the Spectral Dose Index (SDI) method

The gamma radiation of the ground (usually originating from natural and man-made radioisotopes in the top 10 – 20 cm) manifests itself in the gamma ray spectra measured above ground. For airborne measurements with NaI detectors these consists of a background (cosmic radiation, activities in the aircraft and the atmosphere) and of various photopeaks with the corresponding Compton continua. Generally speaking, the higher the total number of counts in the spectrum, the higher the dose rate originating from these radiations. One way to characterize and map the dose rate received on the ground is the Spectral Dose Index (SDI).

The SDI is given by

$$SDI = \sum_{i}^{n} (CR \cdot i) \qquad (1)$$

where CR is the count rate in channel i (i is the channel number). The summation is carried out over n channels, usually above a low-energy threshold (see below).

The total counts must be corrected for various effects (cosmic radiation, aircraft and instrument background, flight height variations). The corrected SDI can be expressed as

$$SDI_{corr} = SDI_{red} \cdot \exp(\mu_{air} \cdot (h - h_{ref})) \qquad (2)$$

Herein SDI_{red} is the SDI corrected for background and cosmic radiation (Sanderson and McLeod 1999); the exponential term accounts for variations in the flight altitude h (with h_{ref} the reference altitude (=100 m) and μ_{air} the attenuation coefficient in air; Bucher 2001).

For taking into account the background and cosmic radiation the following must be considered: the cosmic contribution to the count rate in a given channel i is the product of the

count rate in the high-energy (>3000 keV) cosmic channel (CR_{cosmic}) with the cosmic scattering factor S_i in that channel. Summed up over the whole spectrum this gives

$$SDI_{Cosmic} = CR_{\cos mic} \cdot \sum_{i}^{n} (S_i \cdot i) \qquad (3)$$

The scattering factors can be determined through a measurement flight at different altitude over large lakes; the sum term in (3) can be abbreviated by f_{cosmic} which has a constant value for a given geographical latitude (Bucher 2001).

The background contribution amounts to

$$SDI_{backgr} = \sum_{i}^{n} (CR_{backgr,i} \cdot i) \qquad (4)$$

where $CR_{backgr,i}$ is the background count rate, to be determined from the results of the flight over lakes.

The SDI corrected for background and cosmic radiation is then

$$SDI_{red} = SDI - SDI_{backgr} - SDI_{\cos cmic} \qquad (5)$$

For the summations, a low-energy threshold must be defined. This is a compromise which must take into account on one hand the fact that the low-energy part of the spectrum consists mainly of disturbing counts from Bremsstrahlung and Compton scatter, and that several artificial radioisotopes have typically low energy gamma-lines (e.g. ^{132}Te, 228.2 keV; ^{131}I, 364.5 keV, ^{132}I, 772.6 keV; Murith and Gurtner 1995) on the other. For the present work a threshold energy was taken at 240 keV (Bucher 2001).

Finally, the dose rate DR received at the ground can be given based on the conversion coefficient α:

$$DR_{SDI} = \alpha \cdot SDI_{corr} \qquad (6)$$

But here it must be considered that the cosmic contribution must again be added:

$$DR = DR_{SDI} + DR_{\cos cmic} \qquad (7)$$

The dose rate (nSv/h) originating from cosmic radiation is a function of elevation z (km.a.s.l); for Switzerland the following relationship holds (Murith et Gurtner, 1994):

$$DR_{\cos mic} = 37 \cdot \exp(0.38 \cdot z) \qquad (8)$$

Special flights and measurements have been carried out in Super Puma helicopters to determine the parameters needed for the correction: background, cosmic scattering factors, attenuation coefficient of the air, conversion coefficient SDI – dose rate. The SDI / dose rate conversion coefficient α was determined by comparing airborne and ground measurements (mainly with Reuter-Stokes ionisation chambers). For details see Bucher (2001), the results are given in Table 2.

Table 2. Experimentally determined parameters for ground dose rate mapping in Switzerland (from Bucher 2001). h_{ref} = 100 m, threshold 240 keV

Parameter	Value
SDI_{back}	12'640 s^{-1}
f_{cosmic}	96
μ_{air}	0.0056 ± 0.0002 m^{-1}
α	0.00096 ± 0.00003 $nGyh^{-1}s$

For the conversion of air kerma dose rate ($nGyh^{-1}$) to ambient dose rate equivalent ($nSvh^{-1}$) a factor of 1.2 $nSvh^{-1}$ per $nGyh^{-1}$ is used.

The areal distribution of dose rates, calculated by using the SDI values, is mapped by pixel representations. In the present work the pixel size is 125 x 125 m, which takes into account the average flight elevation that is mainly 100 m and the flight line spacing of 250 m..

6. Procedure to detect and display temporal variations

For a given NPP site the local dose rates (as resulting from the calculated SDI values) are determined first. For each year with survey data a dose rate value grid with 125 m spacing was constructed, corresponding to the survey maps with pixels of same size. Then the grids were limited to the surface area with data coverage over all years. Elevated values within the actual, fenced sites of the nuclear installations have been masked, in order to consider the surrounding environs only.

The net dose rate is calculated by the same procedure as it is applied for the above-mentioned thermoluminescence dose detector arrays (Bucher et al. 2007). For this the local dose rate is splitted into two components 1) local variable part LVP and 2) time-variable part TVP.

The LVP corresponds, for each measurement point x (=pixel), to the difference between the pixel average D(x) over the various (z) annual surveys and the overall average D:

$$LVP(x) = D(x) - D \qquad (9)$$

with $$D(x) = \frac{1}{n}\sum_{z} D(x,z) \qquad (10)$$

and $$D = \frac{1}{m}\sum_{x} D(x) \qquad (11)$$

x

m is the number of pixels and n is the number of annual surveys. The overall time average of LVP is zero.

The time-variable part TVP of the dose rate is calculated from eq. (12)

$$D(z) = \frac{1}{m}\sum_{x} D(x,z) \qquad (12)$$

The sum of LVP(x) and the TVP D(z) gives the expected value E(x,z) for a given measurement point x and survey z:

$$E(x,z) = LVP(x) + D(z) \qquad (13)$$

The net dose rate N(x,z) is calculated according to eq. (14) as the difference between measured and expected value:

$$N(x,z) = D(x,z) - E(x,z) = D(x,z) - D(z) - LVP(x) \qquad (14)$$

The average value of net dose rate is also zero.

The standard uncertainty (variance) of the average dose rate for a given survey is

$$\Delta D(z) = \pm\sqrt{\frac{1}{m-1}\sum_{x}\left(D(x,z) - D(z)\right)^2} \qquad (15)$$

The standard uncertainty (variance) of the average net dose rate, which is zero for the given data, is

$$\Delta N = \pm\sqrt{\frac{1}{(m-1)\cdot(n-1)}\sum_{x,z}\left(D(x,z) - E(x,z)\right)^2} \qquad (16)$$

From the variation of the average net dose rate the limit of recognition for the net dose rate N(x,z) can be determined. For a confidential interval of 95 % the recognition limit RL is

$$RL = 1.645 \cdot \Delta N \qquad (17)$$

Under the assumption that the uncertainty of a net dose rate at the value of the detection limit is similar to the uncertainty of the average net dose rate and a 5 % probability of wrong evidence the detection limit DL is twice the RL:

$$DL = 2 \cdot RL = 3.29 \cdot \Delta N \qquad (18)$$

7. Results

Any change in the average dose rate over the survey years can give hints about trends in a given survey area. Areal averages of the local dose rate in the environs around the power plants KKB, KKG, KKL, and the nuclear facilities PSI and ZWILAG over the survey years are given in Figure 3. The error bars (standard uncertainty, 95 % confidence interval) are also indicated. There is a gap for the area KKB/KKL/PSI/ZWILAG in 2002; in that year only a part of the area could be surveyed for logistic reasons.

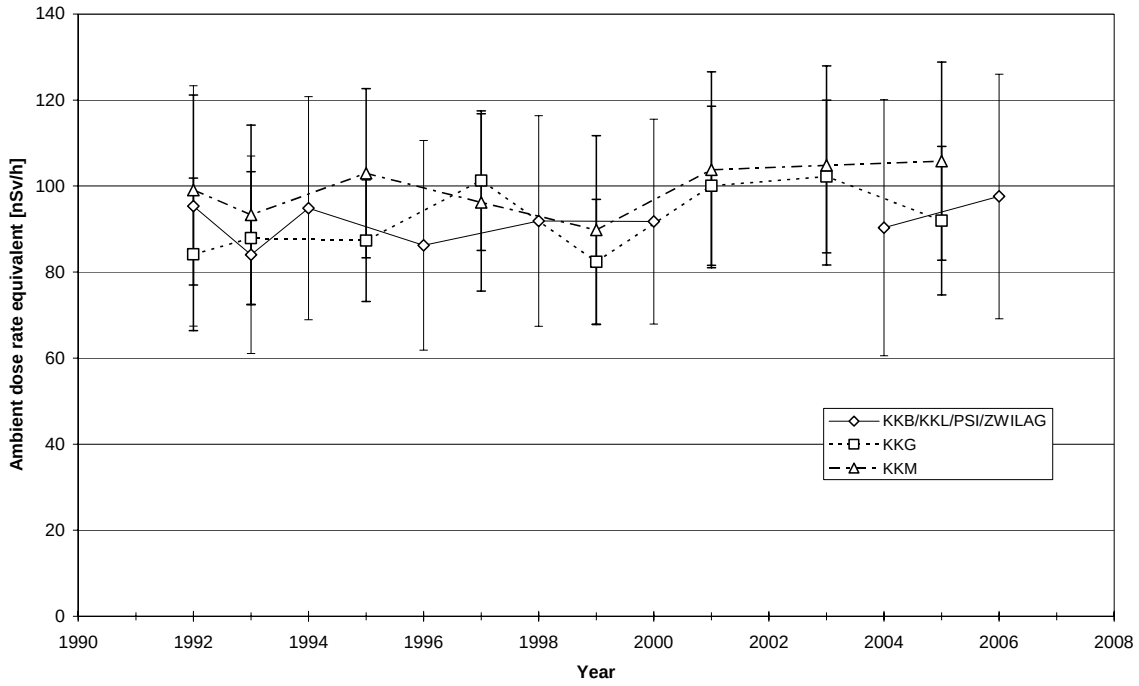

Figure 3: Areal average of local dose rates 1992 – 2005 in the environs of KKG, KKM and KKB/KKL/PSI/ZWILAG with standard error bars (95 % confidence interval).

There are no visible trends in Figure 3, the values remain constant within measurement uncertainties. The error bars are comparable. The areal averages of the net dose rates over the surveyed years plot altogether very close to zero. Also their scatter ranges are limited and comparable, around ±10 $nSvh^{-1}$. As example the results for KKG are given in Figure 4. The results for the other areas look very similar. The scatter of the net dose rates around KKG is the smallest, < 10 $nSvh^{-1}$. Also around KKM the scatter is, with one exception, < 10 $nSvh^{-1}$. There is only one outlier in the KKB/KKL/PSI/ZWILAG area (±19 $nSvh^{-1}$ in 1993); the other values range between 8 and 13 $nSvh^{-1}$.

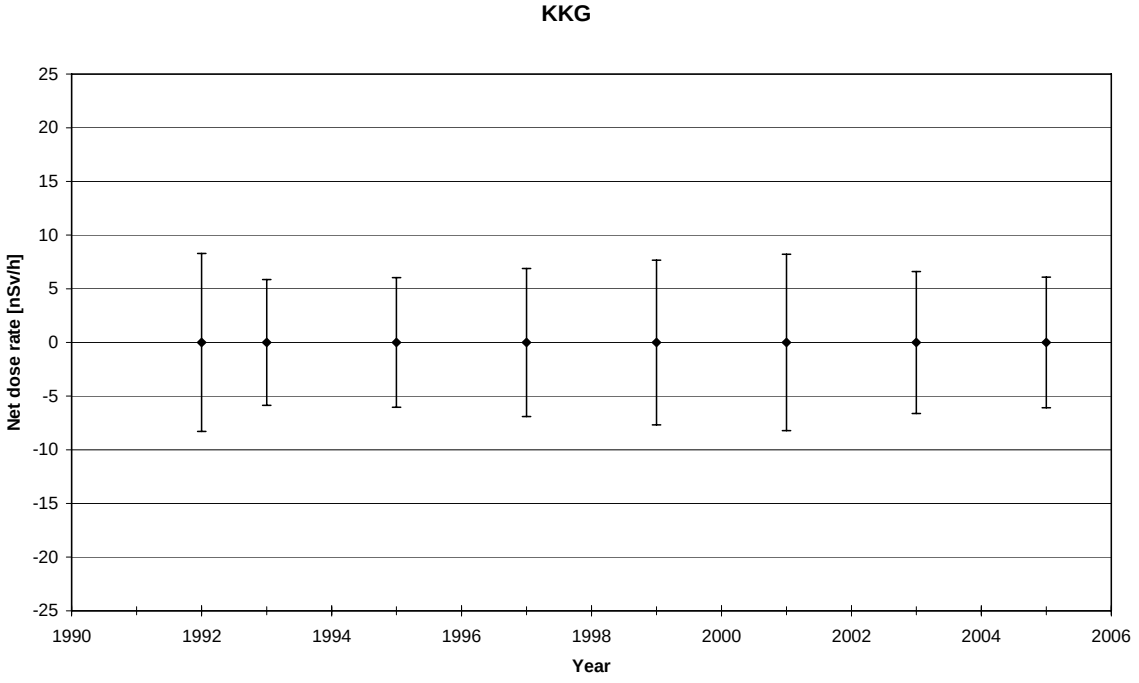

Figure 4: Averaged net dose rates with error bars (95 % confidence interval) in the environs of KKG 1992 – 2005.

The annual airborne gamma spectrometric surveys yield also maps of the artificial radioisotopes ^{60}Co, ^{137}Cs as well as of the Man-made Gross Count Ratio (MMGC, cf. Rybach et al. 2001). MMGC is best suited to detect the presence of artificial radioisotopes like ^{6o}Co, ^{137}Cs. No artificial radioactivity was detectable over the investigated time period outside the fenced areas of the Swiss nuclear installations that could not be explained by nuclear weapon tests or by the Chernobyl event (Rybach et al. 2002). No change in radioactivity levels was observed at the sites over the time span of the surveys.

8. Discussion

The calculated net dose rates and their variation enable to determine the detection limit, see eq. (17) and (18). The numerical values found are 12 nSvh^{-1} for the KKG area, 15 nSvh^{-1} for the KKM area and 20 nSvh^{-1} for the KKB/KKL/ PSI/ZWILAG area. Consequently an additional annual dose of 0.2 mSvh^{-1} could be detected for the KKB/KKL/ PSI/ZWILAG area.

The variance (standard deviation) of the net dose rates in the individual pixels is given in Figures 5-7. For the KKG area there is one location visible with significantly higher variance, see Figure 5. It is located right at a building in Däniken/SO in which an industrial irradiation facility is operated. During the 1995 survey, a net dose rate of 37 nSv/h was detected at that point. This is about three times the detection limit of 12 nSv/h. Due to improved shielding, no elevated values have been found in subsequent years.

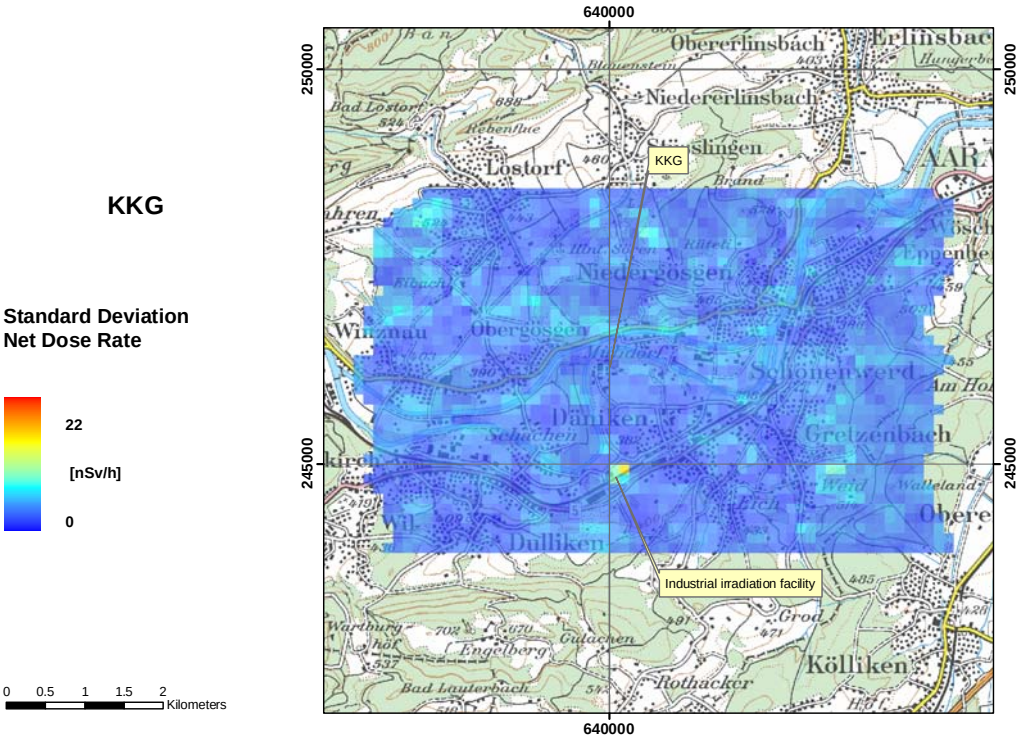

Figure 5: Variance of the net dose rates over the years 1992-2005 in the survey area KKG. Digital maps PK100©2003 swisstopo (DV 316.2)

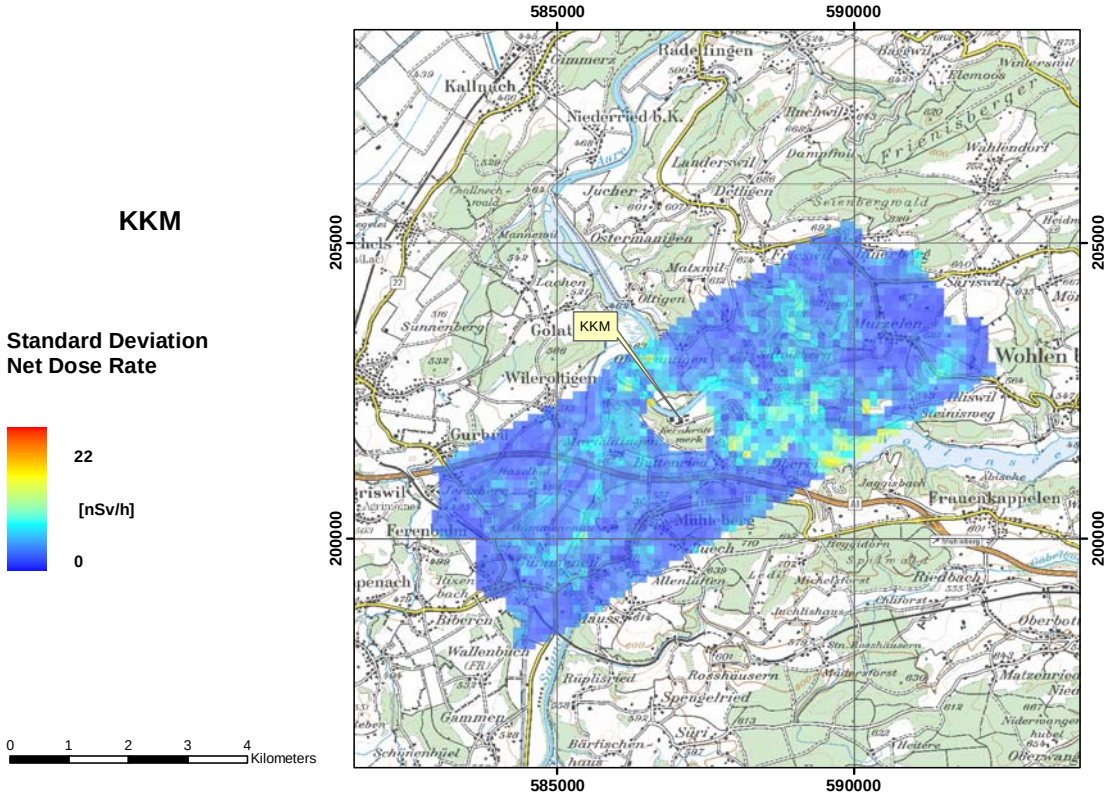

Figure 6: Variance of the net dose rates over the years 1992-2005 in the survey area KKM. Digital maps PK100©2003 swisstopo (DV 316.2)

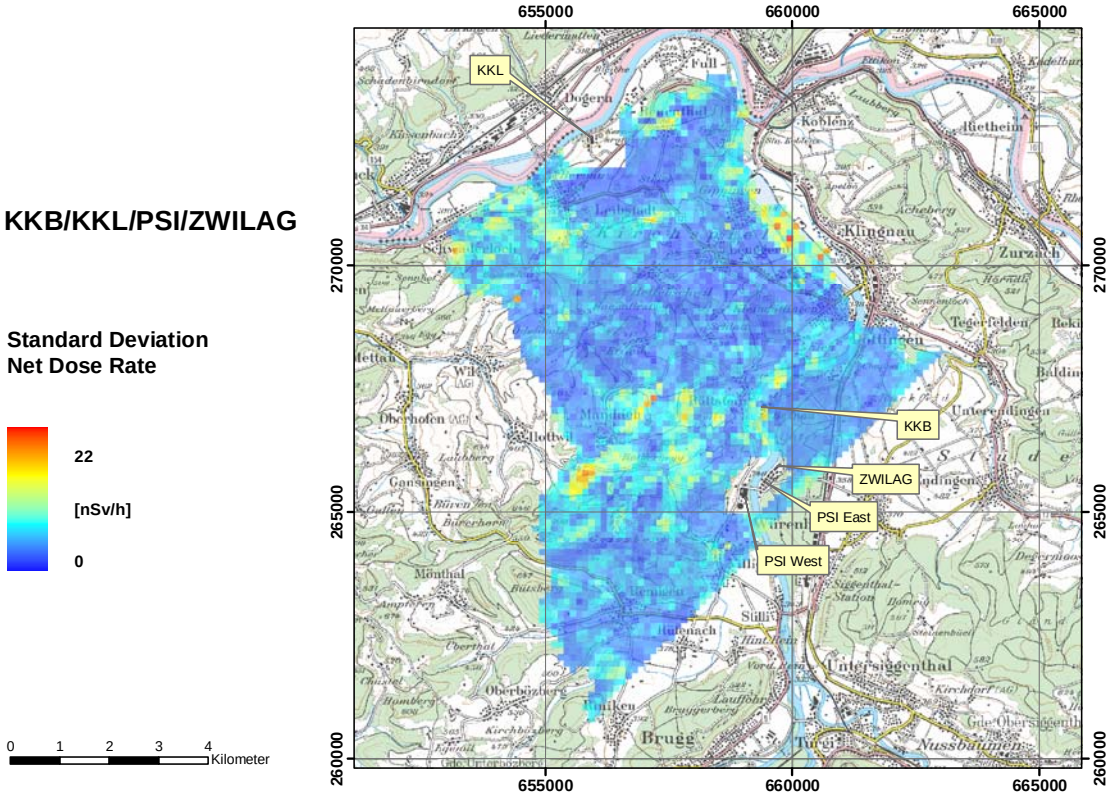

Figure 7: Variance of the net dose rates over the years 1992-2006 in the survey area KKB/KKL/PSI/ZWILAG. Digital maps PK100©2003 swisstopo (DV 316.2)

In the area of KKM (Figure 6), the largest variations are found at the border of the lake Wohlensee. This is due to the limited spatial resolution on one hand and to the limited GPS

positioning accuracy until the year 2000 on the other. Similar features can be found in the KKB/KKL/ PSI/ZWILAG area (Figure 7); they are due to the rivers and lakes present here (reservoir lake Klingnau, river Aare) as well as to relief effects (Jura mountain range).

For the calculations, it is assumed that the survey flight measurements of a particular year were all taken at the same moment. Although this does not influence the results seriously, the effect can be seen in the net dose rates: the histogram of net dose rates of the 2000 survey in the area KKB/KKL/PSI/ZWILAG (Figure 8) shows two separate maxima. They result from the fact that the survey was performed on two separate days. The 2006 survey was flown on one single day; the histogram shows one single maximum.

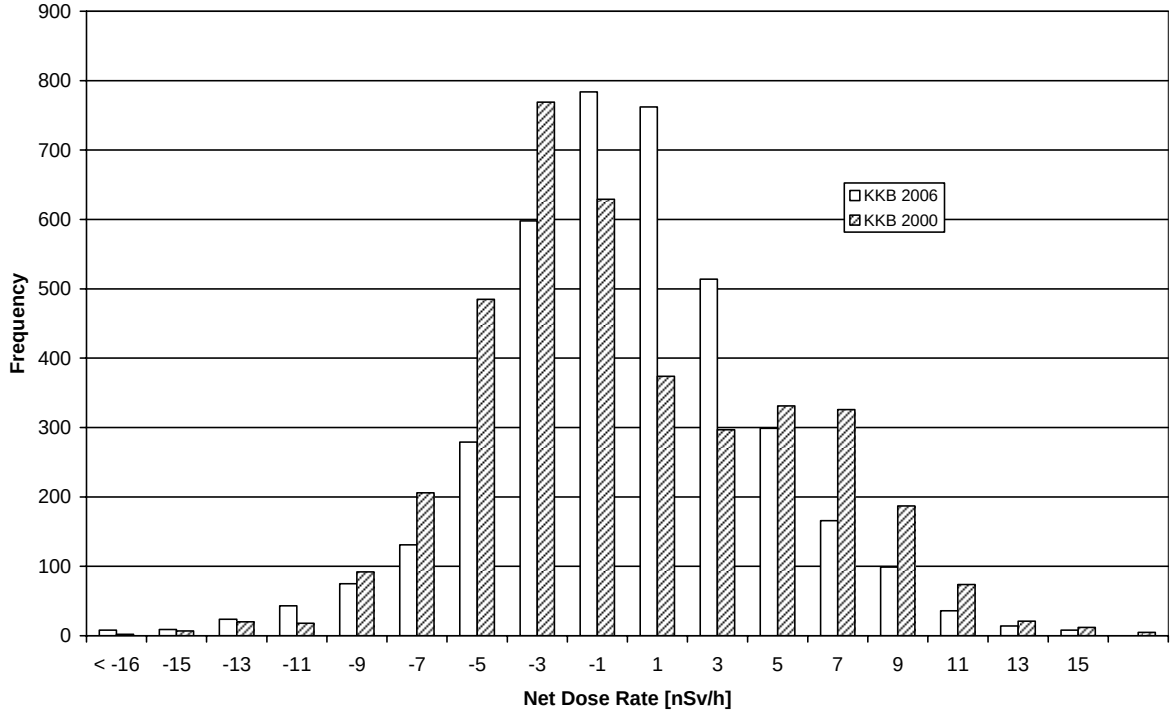

Figure 8: Frequency distribution of net dose rates in the survey area KKB/KKL/PSI/ZWILAG from the 2000 and 2006 surveys.

9. Conclusions

Repeated airborne surveys of the environs of the Swiss nuclear facilities over more than 10 years enable to search for changes of the radiation levels and/or to depict possible trends. Neither the time series of local dose rates nor those of the net dose rates exhibit any such features: the annually repeated measurements show that the radioactivity level in the environs remained constant within measurement uncertainties, i.e. no change in the radiation levels was detected over the last 13 years outside of the fenced sites of the nuclear facilities so far and, especially, no artificial radioactivity was present that could not be explained by nuclear weapon tests or by the Chernobyl event.

The detection limits determined are within the range 12-20 $nSvh^{-1}$. Significant variations in the net dose rate are due to the limited spatial resolution of the survey flight measurements and to the limited GPS position accuracy before the year 2000. This effect is mainly bound to pronounced topographic relief and/or to the borders of surface water like rivers and lakes.

Performing the survey flights on different days in a specific area can create differences in the results; therefore it is advisable to conduct the survey on the same day.

Acknowledgements

We thank the Swiss Federal Nuclear Safety Inspectorate, HSK, Wuerenlingen and the Swiss National Emergency Operation Center, NAZ, Zurich for their continuous support.

10. References

Bucher, B., Cartier, F., Völkle, H., 2007. Blatt 3.4.1 (neu): Bestimmung der Nettodosisleistung mit TLD-Umgebungsdosimetern und automatischen Dosisleistungsmessnetzen. AKU-77/8, Loseblattsammlung FS-78-15-AKU, Empfehlungen zur Überwachung der Umweltradioaktivität.

Bucher, B., Rybach, L.; Schwarz, G., 2000. Environmental mapping: Comparison of ground and airborne gamma spectrometry results under Alpine conditions. In: D.C.W. Sanderson & J.J. McLeod (Ed.): Recent Applications and Developments in Mobile and Airborne Gamma Spectrometry, University of Glasgow, p. 21-18

Bucher, B., 2001. Methodische Weiterentwicklungen in der Aeroradiometrie. Diss. ETH Nr. 13973, 154 p.

Bucher, B., Rybach, L., Schwarz, G., 2005. In-flight, online processing and mapping of airborne gamma spectrometry data. Nuclear Instruments & Methods in Physics Research Section A 540, 495-5001

Murith, C., Gurtner, A., 1994. Mesures in situ et irradiation externe. In: BAG, 1994: Environmental radioactivity and radiation exposure in Switzerland 1993. *Swiss Federal Office of Public Health, Berne*

Murith, C., Gurtner, A., 1995. A guide for in-situ measurements. Bundesamt für Gesundheit, Abteilung Strahlenschutz, Sektion für die Überwachung der Radioaktivität (SUER)

Rybach, L., Bucher. B., Schwarz, G., 2000. Airborne surveys of Swiss nuclear facility sites. In: D.C.W. Sanderson & J.J. McLeod (Ed.): Recent Applications and Developments in Mobile and Airborne Gamma Spectrometry, University of Glasgow, p. 115-121

Rybach, L., Bucher, B., Schwarz, G., 2001. Airborne surveys of Swiss nuclear facility sites. Journal of Environmental Radioactivity 53, 291-301

Rybach, L., Bächler, D., Bucher, B., Schwarz, G., 2002. Radiation doses of Swiss population from external sources. Journal of Environmental Radioactivity 62, 272-286

Sanderson, D., McLeod, J., 1999. European Coordination of Environmental Airborne Gamma Ray Spectrometry. Final Report. European Concerted Action on Environmental AGS. 4th Framework Nuclear Fission Safety Programme.

Schwarz, G.F., 1991. Methodische Entwicklungen zur Aerogammaspektrometrie. Beitraege zur Geologie der Schweiz, Geophysik Nr. 23, Schweizerische Geophysikalische Kommission.

Schwarz, G.F., Rybach, L., 1993. Airborne radiometric survey of the environs of Swiss nuclear installations. Radioprotection, Société Française de Radio-protection, Paris (F), 369-379.

Schwarz, G.F., Rybach, L., Klingelé, E.E, 1995. Data processing and mapping in airborne radiometric surveys. Sciences de la Terre 32, 577-588.

Schwarz, G., Rybach, L., Klingelé, E., 1997. Design, calibration and application of an airborne gamma spectrometric system in Switzerland. Geophysics vol. 62, 1369-1378